

## **Novel Monitoring of Physically-Difficult-to-Access Safeguarded Systems via Autonomous Self-Propagating Space-Filling Chemical Waves**

### **Thomas Dewers**

Nuclear Waste Disposal  
Research & Analysis,  
Sandia National  
Laboratories, Albuquerque,  
NM, USA

### **Jason Heath**

Geomechanics, Sandia  
National Laboratories,  
Albuquerque, NM, USA

### **Kristopher Kuhlman**

Nuclear Waste Disposal  
Research & Analysis,  
Sandia National  
Laboratories, Albuquerque,  
NM, USA

### **Richard Jensen**

Geomechanics, Sandia  
National Laboratories,  
Albuquerque, NM, USA

### **Jacob Harvey**

Geochemistry, Sandia  
National Laboratories,  
Albuquerque, NM, USA

### **Robert Finch**

Internal Safeguards &  
Engagements, Sandia  
National Laboratories,  
Albuquerque, NM, USA

## **Abstract**

The sensing of stimuli including changes or perturbations in spatial and chemical properties is an important operation in monitoring of Safeguarded systems that may be hazardous or impossible to access using conventional remote sensing, sensors, and/or information transmission systems. For example, in chemically reactive or radioactive environments, sensor life may be severely limited due to heat, corrosion, and/or radiation degradation. In other examples, it may be impractical to place sensors and/or transmit information from remote locations simply due to inaccessibility in systems that require sealed containment or inherently have confined spaces such as spent fuel storage facilities or geologic waste repositories. We discuss sensing, analysis, and information transmission using chemical systems with autocatalysis and chemical wave behavior that are used as geospatial environmental sensors and information transmitters. These systems can operate remotely, react to environmental stimuli, and propagate information over large distances, including out of physically-difficult-to-access areas. Application examples include perturbation detection of containment systems such as dry storage canister breaching and detecting changes in fracture network geometries surrounding subsurface repository excavations. The chemical wave sensor systems and methods are applicable in both aqueous and gaseous phases. Computational fluid dynamics simulations including radiolytic and photolytic reactions coupled to transport reveal benefits such as amplifying and/or propagating signals from radiation by-products to where measurements could be made. We report on new benchtop experiments to validate the tuning of traveling chemical waves for sensing radiation by-production over long distances (e.g., > 1 m).

## **Introduction**

International Nuclear Safeguards has the objective of assuring that no nuclear material is diverted to non-peaceful use, which is accomplished through detection, deterrence, and verification (IAEA, 2011). Detection and verification include material accountancy, containment and surveillance, and environmental sampling. Around the globe, dry cask storage of spent nuclear waste is becoming

increasingly important as at-reactor pool storage fills up, and movement of casks can be problematic (NRC, 2006). Deep borehole disposal is being explored as an alternative to underground mined repositories for permanent disposal of spent fuel and other radioactive wastes (Freeze et al., 2016). Both storage and disposal pose unique Safeguards challenges that include poor accessibility. Spent fuel housed in large, heavy casks (e.g., 14-ft long and 150 tons; U.S. NRC, 2017) with radiation, heat, and potentially narrow-to-confined space hazards present difficult and dangerous conditions for verifying seals or detecting potential material diversion. Underground nuclear waste disposal renders materials permanently inaccessible, which can make detecting breaches or intrusion difficult during emplacement and post emplacement.

Radiolytic products in air such as ozone and nitrogen oxides are recognized as markers or indicators of nuclear material (Hecht et al., 2021; Cole et al, 2015). These radiolysis products are typically localized near the ionizing radiation source and can be used for detection of nuclear material. Ozone is amenable to infrared and ultraviolet by standoff optical methods (Hecht et al., 2021). To further leverage radiolytic products as radiation source markers for physically difficult-to-access safeguard applications in both air and aqueous systems, we propose the use of chemical reaction systems or “chemosensors” that exhibit autocatalysis and chemical wave behavior. As discussed herein, chemical waves originate from non-linear coupling of fluid transport and chemical reaction and present as self-sustaining fluctuations in pH, redox state, and/or species concentration (Nicolis and Prigogine, 1977; Ortoleva, 1992). Such “chemosensors”, through the non-linear feedbacks, may amplify signals from the products of ionizing radiation and then propagate those signals spatially and temporally, thus enabling detection of radiation sources in physically difficult-to-access systems with transmission via chemical waves to locations where measurements could be made.

Chemical wave chemosensor systems arguably offer several beneficial components for material accountancy, surveillance-monitoring, and containment verification for Safeguards. We propose that dry cask storage of spent fuel, either in open areas or in a “warehouse”-like environment, are good environments for application and demonstration of our chemosensor concept. Although these examples of containment vary in size and geometry, a few generalities can be made, including (Aymanns and Rezniczek, 2016): the difficulty in verifying seals; problems in accessibility (e.g., by cranes or hoists); “As low as reasonably achievable” or ALARA practices for minimizing exposure and limiting dose; and the large number of casks at any given site and the arduous nature of checking many seals.

The chemical wave chemosensor concept may surmount these issues from the perspective of monitoring. A gaseous or gaseous-aerosol chemical wave system is fully space filling, driven by advective-diffusive transport processes. The precise autocatalytic chemical system can be engineered to be stimulated by chemical perturbations that exist in the gaseous space, such as ionized air and associated byproducts, or on surfaces (examples include powder residues or chemicals released by seal breaching), or even moved or missing casks (by comparing responses over time). A localized excitation of the nonlinear chemical wave system can be distinguishable by the precise perturbation, and the wave motion propagates or broadcasts this messaging through space. With a proper spatial detection system, such as laser spectroscopy or optical methods, the associated excited signals can thus be remotely sensed. We argue that chemosensor systems can be developed to augment current Safeguards methodologies for dry cask storage, and it follows that such a scenario of above-ground or subsurface storage of nuclear waste offers an ideal system for development and demonstration.

This paper thus presents fundamental concepts under development for novel chemical wave chemosensors, including efforts for lab proof-of-concept testing in the gas phase. The chemosensor system may enable a type of “everywhere-at-once” pervasive evaluation of a location. Seals themselves or even applied coatings on casks or other parts of the given system could be designed to be particularly sensitive to damage or disturbances from unauthorized activities of concern to Safeguards, which could then broadcast when contacted by the chemical wave chemosensors.

## Methods: Autocatalysis During Photolytic and Radiolytic Coupled Reactions Numerical

The numerical model we are using in the context of autocatalysis, radiolytic, and photolytic reactions in air is based on the humid air radiolysis model of Wittman (2013), which uses a simplified residence time model to simulate transport and couples bimolecular and termolecular atmospheric reactions with radiolysis terms, for 40 gas-phase species. An application of Wittman’s (2013) model to radiolysis of air around a spent fuel canister is shown in Figure 1 with a decline in dose rate over five hundred years and the corresponding change in air chemistry, with different assumptions about the residence time of the surrounding air.

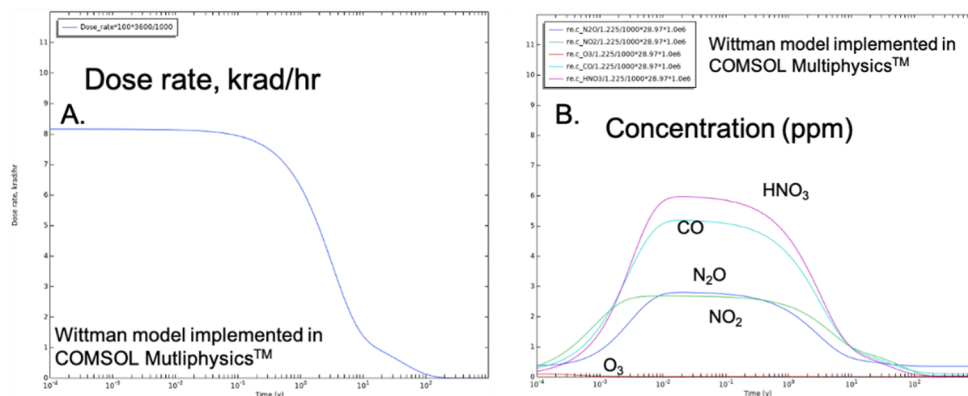


**Figure 1.** Results of COMSOL™ model developed from Wittman (2013) showing model verification by comparison to results of Wittman. A. Dose rate. B. Concentrations of air radiolytic products, which exactly match the results of Wittman (2013; compare to his Figure 3-11).

## Experimental

The construction of a bench-top system for demonstrating behavior of a gas-phase system borrows concepts for experimental testing from the atmospheric sciences, both in the chemical system to be studied and in the mechanics of the experimental design. Behaviors we seek to demonstrate are the following: *information transmission* wherein chemical waves propagate at least one meter in air or air-aerosols; *detection*, wherein chemical waves respond to radiation and/or air ionization by-products characteristic of Safeguarded materials; and *identification and/or quantification*, wherein chemical waves have diagnostic responses. To accomplish this, we have proposed a four-phase experimental approach utilizing a cube-shaped 0.46-m on-a-side benchtop continuously stirred tank reactor (CSTR) coupled to a ~2-meter-long flow tube with a ~0.3 m diameter cross section. This follows from typical designs used in experimental testing for atmospheric kinetics of ultraviolet (UV) photolysis and other reactions occurring in smog (Huang et al., 2017; Gallimore et al., 2017). The precise chemical system being used in our lab experiments is clean dry air with the O<sub>x</sub>-CO<sub>x</sub>-HO<sub>x</sub>-NO<sub>x</sub> system modified slightly

in composition to promote the occurrence of far-from-equilibrium non-linear behavior including temporal oscillations and spatio-temporal chemical waves. We have found via numerical studies (Dewers et al., 2022) that air exposed to UV radiation can generate the required temporal oscillations and chemical wave behavior, and that these chemical waves are modified by exposure to ionizing radiation. Our numerical work is verified by comparison to models in the literature (Wittman, 2013) that were used to study ionization products of air surrounding dry casks used in storage of spent nuclear fuel (and in turn, were validated from high dosage radiation experiments). To build on this numerical work, and to validate the models with lab experiments, we are currently in progress for lab work for the following tiered approach:

- Step 0: a. CSTR with photolysis/simulated (surrogate) radiolysis
- Step 1: CSTR feeding flow tube with UV excitation
- Step 2: CSTR feeding flow tube with +/-UV and +/-O<sub>3</sub>/NO<sub>x</sub> generator point source
- Step 3: Repeat Step 2 but with a surrogate radiation source

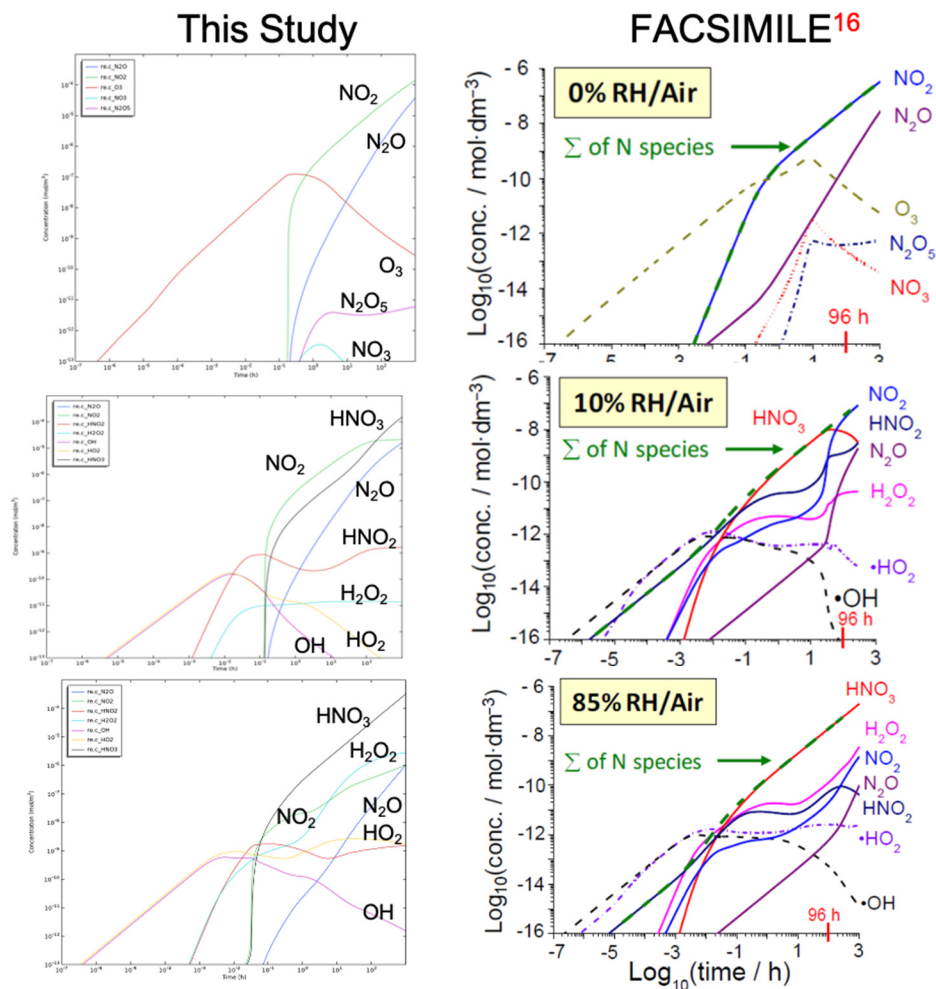
## Results

### Model Verification

As a further test of the COMSOL™ model, we compare our model runs to those of Morco (2020) examining gamma radiolysis of humid air, at 75°C and a dose rate of 1 Gy/h (Figure 2) using the radiolysis code FACSIMILE. The COMSOL™ model does a good job reproducing the changing speciation at increasing humidity (from 0, 10, and 85% relative humidity) and a reasonable job at matching the concentrations. This suggests our COMSOL™ model is well adapted to describe humid air radiolysis at a range of temperature, radiation, and humidity conditions.

For our chemosensor development, we are interested in coupling the above chemical and radiolytic kinetics with photolytic kinetics, as many of the gas-phase oscillatory systems investigated in atmospheric sciences are driven by UV photolysis. To the Wittman-verified COMSOL™ model, we add 20 photolytic reaction rates as given in the Burkholder et al. (2021) compilation. The wavelength dependence and the varying intensity of UV sources should allow a wide range of “tuning” the resulting nonlinear rates, and, it follows, the oscillatory behavior, chemical wave behavior, and response when coupled to radiolysis. This may allow an ability to tune a chemical wave chemosensor to be able to discern between sources of radiolytic yield, one of the goals of our Safeguards research.

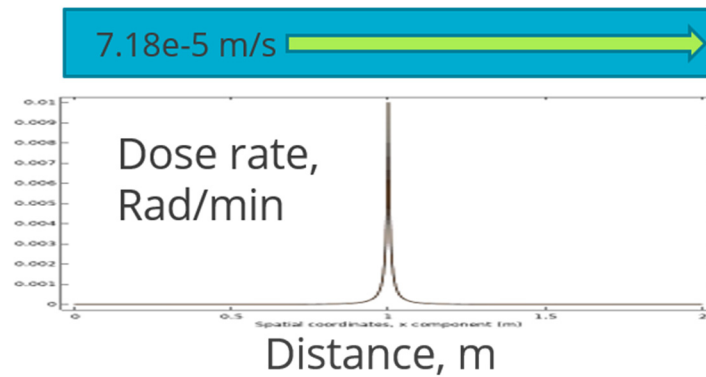
To numerically demonstrate the occurrence and sensitivity of this gas-phase system to the development of spatially propagating chemical waves, we couple the CSTR system to a “flow tube”, wherein the reactor effluent is fed into a numerically modeled 15.25-cm (6-inch) square cross section fused-quartz or Teflon tube that is approximately 2-m in length (Figure 3). The flow tube allows us to demonstrate chemical wave behavior in a quasi-one-dimensional spatial format (i.e., 1D wave propagation and flow). The design here includes a surrogate radiation source to be located at the center of the tube, utilizing an O<sub>3</sub>-NO<sub>x</sub> source at the tube longitudinal center, to demonstrate the wave behavior as perturbed by a radiation source. The choice of fused quartz glass or Teflon is associated with the particular UV transmissivity that is required to excite the required photolytic reactions in the nonlinear chemical wave reaction network.



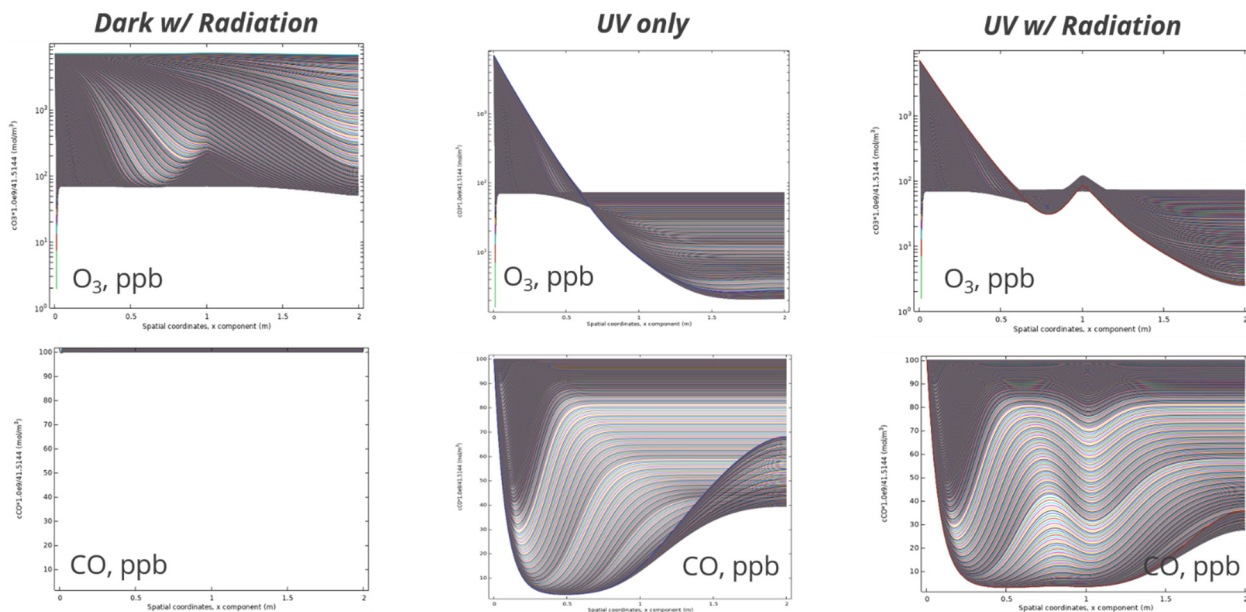
**Figure 2.** Comparison of COMSOL humid air radiolysis model to that of FACSIMILE model as used by Morco (2020). The results do not exactly match but the speciation with changing relative humidity matches very closely.

Both quartz and TFE Teflon are used in atmospheric reaction kinetic studies involving UV photolysis. A 1D numerical model of this system shows the expected behavior under different environmental conditions (Figure 4). The “dark” condition just involves bimolecular and termolecular reaction, the UV condition includes these plus photolytic reactions sensitive to the precise UV wavelength, and the UV-with-radiation condition includes all of the above plus radiolysis kinetics sensitive to the dose rate and precise radionuclide(s). The dark example shows ozone concentration slowly increasing with time with successive diffusion-dispersion profiles. The UV-only and UV-with-radiation examples display chemical wave behavior, propagating from left to right in the successive time profiles. The UV-plus-radiation example shows the influence of the point source of radiation (as shown in Figure 4), and how the information contained in the chemical wave is transmitted to the tube effluent side by the propagating chemical wave. This behavior is what we endeavor to capture with our experimental design and our lab proof of concept experiments.

### Flow Tube, 6" square



**Figure 3.** One-dimensional model for the flow-tube design, with effluent from the CSTR entering the left-hand side of the tube, and tube effluent on the right-hand side. A surrogate radiation source is located at the center-point of the tube, such that wave behavior upstream of the source would act as an unperturbed wave system, and wave behavior downstream of the source demonstrates the same system as influenced by the surrogate radiation source. The flow rate is equivalent to 2 L/min.



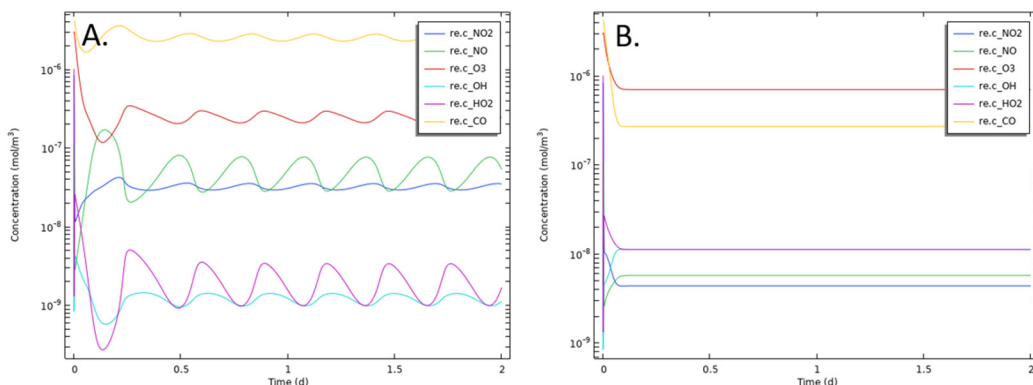
**Figure 4.** Simulations of the  $O_x$ - $OH_x$ - $CO_x$ - $NO_x$  chemical system in a flow tube system with profiles shown at every time step. From left to right the panels include: dark reaction kinetics (no photolysis and no radiolysis); UV only (photolysis but no radiolysis) and UV + radiation (photolysis and radiolysis). The UV-only and UV w/ radiation examples (right-hand side) show development of a propagating chemical wave, from left to right, most evident in the CO profiles.

Figure 5 shows a model of a continuously stirred tank reactor (CSTR) system that can be employed at benchtop scale with compositions of constituents of concern (e.g., ozone, CO,  $NO_x$ ) at levels that pose no hazards associated with reactor effluent into air, with use of a fume hood to vent reactor



effluent under normal hood air flow. Exposure to UV radiation with wavelengths in the range of 250 to 350 nm show well developed temporal oscillations with a period of approximately six hours, which is amenable to lab monitoring methods (Figure 5A). Under exposure to air ionization at relatively high dose rate of 1 Gy/hr, Figure 5B shows that the ionization products quench the oscillatory behavior, demonstrating a sensitivity of the chemical wave system to a radiation source.

This model suggests an experimental design we explore further below, for the CSTR, involving: a source for clean dry air; sources of additional CO<sub>x</sub>, NO<sub>x</sub>, and O<sub>3</sub> (using a generator that uses air and NO<sub>2</sub> canisters as sources); a gas mixing manifold; a source for humidity (a simple heated flask with water, or using salt mixtures); a central chamber with UV sources of varying wavelengths; and gas analyzers attached to the CSTR effluent side. This is similar to the atmospheric chamber design discussed by Gallimore et al. (2017).



**Figure 5.** A. Nonlinear oscillatory behavior in the O<sub>x</sub>-OH<sub>x</sub>-CO<sub>x</sub>-NO<sub>x</sub> system for a CSTR system with reactor feed at rate of 2 L/min. Under these conditions (including inlet concentrations) the system displays oscillations with period of ~ 6 hours. B. Same system as (A), perturbed by gamma radiation. Kinetics follow the laboratory results for a <sup>60</sup>Co source measured through glass, for ozone generation in flowing air after Gerasimov (2004).

### Atmospheric Reactor System Design

Based on the numerical modeling studies, we designed and built a bespoke CSTR and flow tube reactor system with tunable UV-LEDs (Figure 6). The windows of the CSTR and the flow tube are made of Teflon. The heat sinks for the CSTR (Figure 6A) and the flow tube (Figure 6B) hold a total of 513 UV-LEDs that cover the specific wavelengths of 405, 395, 385, 375, 365, 340, 325, 310, 295, 275, and 265 nm, which fall in UV-A (315-400 nm), UV-B (280-315 nm) and UV-C (100-280 nm) bands. Each wavelength has multiple LEDs that are connected to a dimmable power supply thus giving us the ability to tune the spectrum shone into the CSTR and the flow tube reactor—the original design for the choice and number of LEDs was based on simulating as a baseline the ASTM solar standard G173-03 as implemented in Gueymard (2005). Furthermore, the system includes two 222 nm excimer bulbs to allow stimulation of the chemical reactions in the far UV-C and to potentially act as a surrogate radiation source. The system includes ozone and nitrogen oxide generators and measuring instruments. Experiments are currently underway to test creation of temporal and spatial chemical oscillations and waves and their response to surrogate radiation, including for the approximately 2-meter traveling distance as that may be useful to transmit signals from physically-difficult-to-access areas where optical/laser measurements could be made in a real scenario. An example of the UV irradiance and NO photolysis is shown in Figure 7.

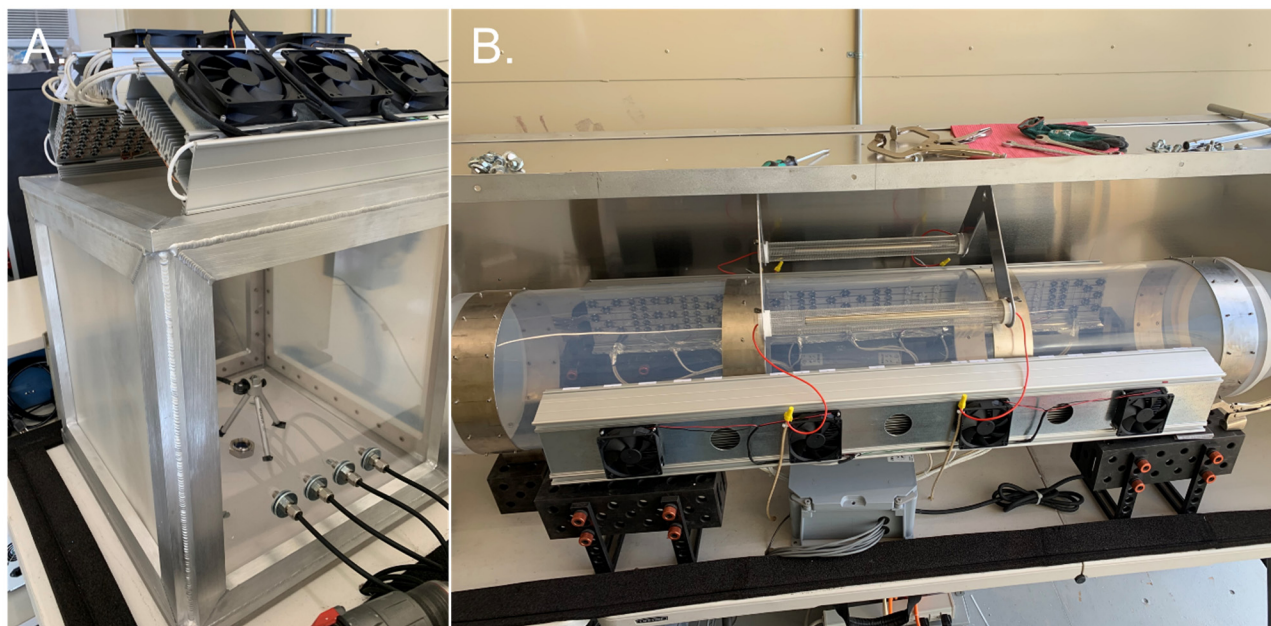


**Figure 6.** Atmospheric chemical wave testing system. A. Continuously stirred tank reactor with cube shape of 0.46 m on a side. Heat sinks with UV-LEDs are on top. A spectroradiometer holder is visible inside the chamber. B. Flow tube reactor at approximately 2.6 m including the diffuser cones on the ends. Heat sinks with UV-LEDs are on the sides and positioned opposite each other. 222 nm excimer bulbs are visible near the top middle of the tube. The left diffuser cone (not fully visible in B) is meant to support linear and laminar Poiseuille flow. Not shown are the power supply bank and control switches to power each UV-LED wavelength separately.

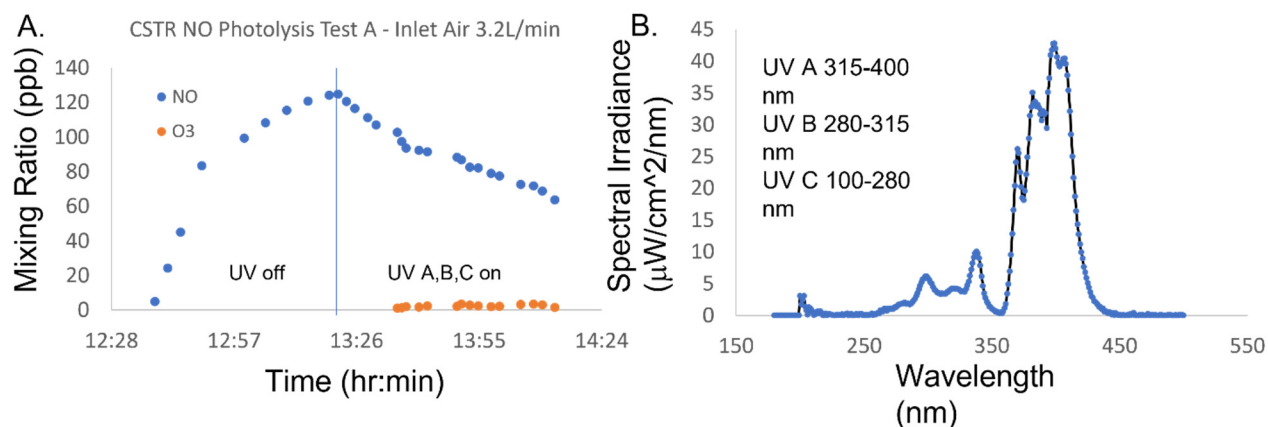


**Figure 7.** A. NO photolysis experiment performed as part of scoping study of the reactor system shown in Figure 6. NO (blue dots) is fed from the calibration device at a known flow rate and concentration which enables calculation of the residence time distribution function of the CSTR. At about 13:00 hours, the LED UV system is turned on, which results in NO photolysis with O<sub>3</sub> as a byproduct (orange dots). B. Spectral irradiance measured inside the CSTR, which results in the photolysis in A.



## Conclusions

Through a series of increasingly complex simulation schemes for batch-mode, CSTR, and spatiotemporal dependent chemical reactive transport, we demonstrate the use of nonlinear chemical waves as geospatial sensors. Attributes of this sensing capability include: 1) chemical compounds expressing as temporal and/or spatial oscillations in concentration due to nonlinear feedback in reactants and products, hereafter called chemical waves; 2) the chemical waves are spacing-filling; 3) the frequency, amplitude, and spatial patterns of chemical waves are triggered by characteristics of the host medium (e.g., trace amounts of solid, gaseous, or liquid chemical compounds; physico-acoustic perturbations; radiation; magnetic fields; and optical stimulation); 4) the chemical waves transmit information on triggering sensed quantities via chemical wave trains; 5) chemical wave trains are read-out by concentration measuring methods; and 6) the chemical waves patterns are tuned for identifying radiation and/or radiolytic byproducts. Chemical waves respond to and retain a history of encountered stimuli, and the waves propagate spatially even in the absence of advection. The applied chemical compounds sense characteristics of a host medium (which could be gas or liquid phase) by producing diagnostic spatial and temporal patterns in chemical waves as triggered by what is in the host medium that is contacted by the chemicals. The chemical waves perform *in materia* analysis at different levels of complexity and at non-toxic concentrations depending on the particular system and application, which may include future uses such as: identification of particular substances or configurations of items in the host medium; verification that seals or other features have not been damaged or removed; and/or verification that containers have not leaked a substance of interest.

## Acknowledgements

The authors thank the US DOE National Nuclear Security Administration, Office of Defense Nuclear Nonproliferation Research and Development, for funding this work. This paper describes objective technical results and analysis. Any subjective views or opinions that might be expressed in the paper do not necessarily represent the views of the US Department of Energy or the United States Government. Sandia National Laboratories is a multimission laboratory managed and operated by National Technology & Engineering Solutions of Sandia, LLC, a wholly owned subsidiary of Honeywell International Inc., for the U.S. Department of Energy's National Nuclear Security Administration under contract DE-NA0003525. SAND2023-03507C.

## References

- Aymanns, K., Rezniczek, A. 2016. Report on a meeting on “Use of passive sealing systems for casks in spent fuel storage facilities in Germany.” CS WG Meeting, Ispra, Nuclear Waste Management, IEK-6.
- Burkholder, J.B., Sander, S.P., Abbatt, J., Barker, J.R., Huie, R.E., Kolb, C.E., Kurylo, M.J., Orkin, V.L., Wilmouth, D.M., Wine, P.H. 2015. Chemical Kinetics and Photochemical Data for Use in Atmospheric Studies, Evaluation No. 18, JPL Publication 15-10, Jet Propulsion Laboratory, Pasadena, accessed 11-1-2021, <http://jpldataeval.jpl.nasa.gov>.
- Cole, J., Su, S., Blakeley, R.E., Koonath, P., Hecht, A.A. 2015. Radiolytic yield of ozone in air for low dose neutron and x-ray/gamm-ray radiation. *Radiation Physics and Chemistry* 106, 95–98.
- Dewers, T.A., Heath, J.E., Kuhlman, K.L., Jensen, R.P., Finch, R.J., Harvey, J.A. 2022. Safeguards Assessments via Nonlinear Chemical Waves for Sensing and Information Transmission. SAND2022-0643, Sandia National Laboratories, Albuquerque, NM, 32 p.

- Freeze, G., Stein, E., Price, L., MacKinnon, R., Tillman, J. 2016. Deep Borehole Disposal Safety Analysis. Prepared for U.S. Department of Energy Used Fuel Disposition, FCRD-UFD-2016-000075, Rev. 0, SAND2016-10949R.
- Gallimore, P.J., Mahon, B.M., Wragg, F.P.H., Fuller, S.J., Giorio, C., Kourtchev, I., Kalberer, M. 2017. Multiphase composition changes and reactive oxygen species formation during limestone oxidation in the new Cambridge Atmospheric Simulation Chamber (CASC), *Atmos. Chem. Phys.* 17, 9853-9868.
- Gerasimov, G.Y. 2004. Radiation-chemical formation of ozone in an oxygen-containing gas atmosphere. *High Energy Chemistry* 38, 75-80. Translated from *Khimiya Vysokikh Energii*, Vol. 38, No. 2, 2004, pp. 101–106.
- Gueymard, C.A. 1995. SMARTS2, A simple model of the atmospheric radiative transfer of sunshine: Algorithms and performance assessment, Prof. Paper FSEC-PF-270-95. Florida Solar Energy Center, 1679 Clearlake Road, Cocoa FL.32922.
- Hecht, A.A., Galo, R., Fellows, S., Baldez, P., Koonath, P. 2021. Radiolytic ozone yield  $G(O_3)$  from  $^{210}Po$  alpha-particle radiation in air. *Radiation Physics and Chemistry*, 183, 109387, <https://doi.org/10.1016/j.radphyschem.2021.109387>.
- Huang, Y., Coggon, M.M., Zhao, R., Lignell, H., Bauer, M.U., Flagan, R.C., Seinfeld, J. 2017. The Caltech photooxidation flow tube reactor: Design, fluid dynamics, and characterization, *Atmos. Meas. Tech.* 10, 839-867.
- IAEA. 2011. Safeguards techniques and equipment: 2011 edition. IAEA International Nuclear Verification Series No. 1 (Rev. 2), 162 p.
- Morco, R.P. 2020. Gamma-Radiolysis kinetics and its role in the overall dynamics of materials degradation. Ph.D. Thesis, The University of Western Ontario, 250p.; FACSIMILE Model found at <https://www.mcpa-software.com/radiolysis-model>, accessed 11-7-2021.
- National Research Council. 2006. Safety and Security of Commercial Spent Nuclear Fuel Storage: Public Report. Washington, DC: The National Academies Press. <https://doi.org/10.17226/11263>.
- Nicolis, G., Prigogine, I. 1977. *Self-Organization in Nonequilibrium Systems: From Dissipative Structures to Order through Fluctuations*, John Wiley and Sons, New York, 491 p.
- Ortoleva, P.J. 1992. *Nonlinear Chemical Waves*. Wiley and Sons, New York, 302 p.
- U.S. Nuclear Regulatory Commission. 2017. Safety of spent fuel storage. NUREG/BR-0528, 16 p.
- Wittman, R. 2013. Radiolysis model sensitivity for a Used Fuel Storage Canister, Pacific Northwest National Laboratories PNNL-22773, 48p.